WATER WAVE RUN-UP ON A BEACH, II

Joseph B. Keller and Herbert B. Keller
Courant Institute of Mathematical Sciences
New York University

Consultants for

Service Bureau Corporation
New York, N.Y.

1. Introduction

In a previous report [1], we presented the results of our investigation up to June, 1964 of waves incident upon a beach. Particular emphasis was placed on the wave height at the undisturbed shore-line and the motion of the shoreline, including the maximum run-up distance. For time harmonic waves of small amplitude incident from the open sea, formulas for these quantities were derived based upon the linear theory of water waves. The nonlinear theory was used to find the range of validity of these formulas. In addition a numerical method was devised for the calculation of the wave motion on the basis of the nonlinear shallow water theory. This method was applied to waves on a uniformly sloping beach. The results showed fair agreement with the analytical results for waves of low frequency but not for higher frequencies.

From June 1964 to June 1965 we have improved the numerical method by using a finite difference scheme of higher order accuracy described in section 3 of this report. With the improved method we have made extensive calculations which agree much better with the analytical results and which do so up to higher frequencies. However the discrepancies between the numerical and analytical results still occur at frequencies somewhat below those at which the analytical results cease to be valid. Although we have not found the cause of these discrepancies, we can conclude that at the lower frequencies the numerical results are reliable. Some of the results are described in section 5 of this report.

We have also developed the analytical theory of wave breaking and bore formation and growth on a uniformly sloping beach. This theory is based upon the nonlinear shallow water theory. By employing the method of characteristics in section 6 we determine how an incident wave becomes distorted and finally reaches the breaking point. Then in section 7 we utilize the theory of weak shock waves to determine how the bore forms and grows. This analysis, being based on the hypothesis that the wave is weak, cannot yield all the properties of the bore, especially those at the shoreline. Nevertheless it does determine how the height of the bore increases rapidly at first and then more gradually. It also determines the position and speed of the bore as functions of time.

This theory of bore formation and growth on a sloping beach should form the basis of further theoretical and numerical investigations of water wave run-up.

2. Review of analytical results

In order to compare our present numerical results with our previous analytical ones, we shall first review the analytical results contained in our previous report. It is convenient to present those results in terms of the dimensionless variables which we have used in the numerical work. These dimensionless variables are the time, t, the horizontal distance x measured from the undisturbed shoreline, the undisturbed water depth $H(x)$, the disturbed water depth $h(x,t)$, the shoreline position $\xi(t)$ and the horizontal water velocity $u(x,t)$. They are related to the corresponding dimensional quantities $\bar{t}$, $\bar{x}$, $\bar{H}$, $\bar{h}$, $\bar{\xi}$ and $\bar{u}$ by the scaling relations

$$\bar{x} = x\, D \cot \alpha, \quad \bar{h} = h\, D, \quad \bar{H} = H\, D$$

1. $$\bar{t} = t(D/g)^{1/2} \cot \alpha, \quad \bar{u} = u(gD)^{1/2}, \quad \bar{\xi} = \xi\, D \cot \alpha$$

Here α is the beach angle at the undisturbed shoreline $x = 0$ and D is a vertical length scale factor. It is to be noted that the horizontal length scale factor is $D \cot \alpha$. See Figures 1a and 1b.

We have found it convenient to choose D so that the dimensionless undisturbed water depth H is unity at $x = -1$. In addition the undisturbed depth is zero at the undisturbed shoreline. Thus $H(x)$ must satisfy the two conditions

2. $$H(0) = 0, \quad H(-1) = 1$$

It is assumed that the water lies to the left of the undisturbed shoreline in the region $x < 0$ before the disturbance arrives. For a uniformly sloping bottom profile, the dimensionless undisturbed depth is simply

3. $$H(x) = -x.$$

Let us assume that the incident wave height $[h(x,t)-H(x)]_{inc}$ in the deep water far from shore, i.e., in the region $x \ll -1$, is given by a periodic sinusoidal wave

4. $$[h(x,t)-H(x)]_{inc} = a\cos(\omega t-\beta x)$$

Here the dimensionless angular frequency ω, the dimensionless wave number β and the dimensionless amplitude a occur. They are related to the dimensional angular frequency $\bar{\omega}$ and amplitude $\bar{a}$ by the relations

5. $$\omega = \bar{\omega}(D/g)^{1/2}\cot\alpha, \quad a = \bar{a}/D, \quad \beta = \bar{\omega}^2 g^{-1} D \cot\alpha = \omega^2\tan\alpha.$$

The amplification factor A is defined as the ratio of the maximum water depth at the undisturbed shoreline to the amplitude of the incident wave far from shore. Thus

6. $$A = \max_t |h(0,t)/a|$$

We have previously determined A for water of slowly varying depth. This means water for which the fractional change of depth in a wavelength is small except near the shoreline. When this condition is satisfied and $\lim_{x\to-\infty} H(x) = 1$, we find that A depends only upon ω and α and is given by

7. $$A(\omega,\alpha) = \sqrt{\frac{2\pi}{\alpha}}\left(\tanh z + \frac{z}{\cosh^2 z}\right)^{1/2}$$

Here z, a function of $\omega^2\tan^2\alpha$, is the positive root of the equation

8. $$z\tanh z = \omega^2\tan^2\alpha$$

In this case it is not required that $H(-1) = 1$ since D is chosen as the undisturbed depth at $x = -\infty$. Graphs of A as a function of ω for various beach angles α, based upon (7), are given in Figures 3 and 7. The limit of $A(\omega,\alpha)$ as α tends to zero is easily found to be

9. $A(\omega,0) = \sqrt{4\pi\omega}$

Since the result (9) applies when ω is fixed, it follows from (5) that $\bar{\omega}$ tends to zero as α does. Therefore (9) is the asymptotic form of (7) for low frequencies $\bar{\omega}$.

The result (7) was obtained in two ways. First it was deduced from the linear theory of water waves in water of any depth. Then it was rederived by matching the result of the linear theory in deep water to the result of the non-linear shallow water theory employed near the shore. The latter derivation also yields a limitation on the incident amplitude for the result to be valid. It implies that the amplified wave height be small compared to the wavelength. Analytically the condition is

10. $$a \leq a_{max} \equiv \frac{1}{\omega^2 A(\omega,\alpha)}$$

Here A is given by (7). Graphs of this limiting amplitude as a function of ω are shown in Figure 4 for various values of α.

The result (9) was also derived in another way. It was shown to be the high frequency asymptotic form of the amplification given by the linear shallow water theory in water of arbitrarily varying depth. Thus the result (7), which is valid for high frequency waves, has a low frequency asymptotic form which is the same as the high frequency asymptotic form of the result of the shallow water theory, a theory which is valid for low frequencies. This shows that the two results are asymptotically equal in some intermediate frequency range, as one should expect and that the two results supplement each other.

For very low frequencies, the linear shallow water theory yields

11. $A = 2 + 2\omega^2 b + \dots$

Here b is defined by

12. $$b = \int_0^\infty x\left[H^{-1}(x) - H^{-1}(\infty)\right] dx$$

In the special case of a piecewise linear bottom profile, the equations of the linear shallow water theory can be solved explicitly for all frequencies. We have considered the special case in which

13. $$H(x) = -x, \quad -1 \leq x \leq 0$$
$$= 1, \quad x \leq -1$$

In this case the amplification is given by

14. $$A(\omega,\alpha) = 2\left[J_0^2\left(2\omega \frac{\tan\alpha}{\alpha}\right) + J_1^2\left(2\omega \frac{\tan\alpha}{\alpha}\right)\right]^{1/2}$$

Here J_o and J_1 are Bessel functions of orders zero and one respectively. This function agrees with (11) for small values of ω and with (9) for large values of ω. A graph of A based on (14) is shown in Figure 3 for $\alpha = 0$. It is clear from (14) that when α is small, A is practically independent of α.

On the basis of all of the preceding results, we can formulate an over-all description of the amplification as a function of frequency and beach angle. At zero frequency the amplification is two and then it increases quadratically with the frequency as is shown in (11). It continues to increase (see Figure 3) in a undulatory manner as is shown by (14), with an undulation frequency determined by the horizontal scale of the bottom profile. It undulates about the curve $A = (4\pi\omega)^{1/2}$, which it approaches as ω increases. Then the amplification continues increasing at the slower rate given by (7). This latter transition shows that as the water depth becomes appreciable compared to the wavelength, it has the effect of diminishing the amplification.

The gradual increase of amplification with frequency just described applies only until bore formation occurs. The amplitude at which this occurs for any given frequency is given by (10).

A quantitative theory of amplification and run-up when bores form has not yet been developed.

3. Formulation of the general problem

The finite difference calculations are based on the same nonlinear shallow water theory formulation presented in [1], which we repeat here for completeness.

In terms of the variables (1.1) the mass conservation equation is

1. $$h_t + (uh)_x = 0,$$

and the linear momentum conservation equation is

2. $$u_t + uu_x = (H-h)_x .$$

If the location of the shoreline at time t is denoted by $x = \xi(t)$, then since the water depth there is always zero we have

3. $$h[\xi(t),t] = 0.$$

In addition the velocity of the shoreline must be equal to the water velocity at the shoreline so

4. $$\frac{d\xi(t)}{dt} = u[\xi(t),t].$$

Equations (3) and (4) are boundary conditions which must be satisfied on the moving shoreline.

We shall consider the motion only in the interval $-1 \leq x \leq \xi(t)$ for $t > 0$ since we assume that known (subsonic) waves are incident from $x < -1$ for all $t > 0$. If the local sound speed is denoted by $c \equiv \sqrt{h}$ then (1) and (2) can be written in characteristic form as

5. $$(u + 2c)_t + (u + c)(u + 2c)_x = H_x$$

6. $$(u - 2c)_t + (u - c)(u - 2c)_x = H_x.$$

Equation (5) determines $(u+2c)$ along the "positive" characteristics, $dx/dt = u+c$, which, as t increases, enter $x > -1$ from $x < -1$. If the linear shallow water theory were valid for $x < -1$ and $H(x) = \text{const} = 1$ there, then the general solution would be

$$u = F(t-x) + f(t+x),$$

$$h - 1 = F(t-x) - f(t+x).$$

In the linear theory we use $c = \sqrt{h} = 1 + (h-1)/2$ and so

$$u(x,t) + 2c(x,t) = 2\left[1+F(t-x)\right].$$

Clearly the function F in this equation represents the incident part of the linearized wave motion. Thus we take for the boundary condition to be imposed at $x = -1$:

7. $$u(-1,t) + 2c(-1,t) = 2\left[1 + F(t-1)\right]$$

The water is to be at rest initially so that

8. $h(x,0) = 0, \quad u(x,0) = 0 \quad \text{in } -1 \leq x \leq \xi(0) = 0.$

Our problem is thus: to solve (1) and (2) for $u(x,t)$ and $h(x,t)$ in $-1 \leq x \leq \xi(t)$ for $t > 0$, subject to the conditions (3) and (4) on the unknown boundary $x = \xi(t)$, the condition (7) on $x = -1$ and conditions (8) at $t = 0$. The shoreline position $\xi(t)$ must be determined simultaneously. We shall study only motions in which bores are not present.

4. Finite difference scheme.

The numerical method which we employ is of higher order accuracy then the one previously employed in [1] and is based on the Lax-Wendroff scheme [2]. Again we use a uniform spatial net, $x_j = j\Delta x$ and possibly non-uniform time net, $t_{k+1} = t_k + \Delta t_k$. The computed shoreline position at time t_k is denoted by $\xi_k = \xi(t_k)$ and then $x_{s(k)}$ is defined as the net point for which

1. $$x_{s(k)} + \frac{\Delta x}{2} < \xi_k \leq x_{s(k)} + \frac{3\Delta x}{2} .$$

The calculations at time t_{k+1} are then divided into four kinds for four different types of net points, as follows:

I) interior points: $x_1 \leq x_j < x_{s(k)}$,

II) shoreline interior points: $x_j = x_{s(k)}$,

III) incident wave: x_0,

IV) shoreline: ξ_{k+1}.

At points of type I and II (see Figures 8a,b) we use high order accuracy difference approximations of the equations of motion (3.1), (3.2). Rather than write down the messy difference equations, which are not instructive, we shall indicate the expansions from which they are easily deduced: Thus at any point P of Figure 8a or 8b an application of Taylor's theorem yields

$$h(P) = h(P') + \Delta t\, h_t(P') + \frac{\Delta t^2}{2} h_{tt}(P') + O(\Delta t^3),$$

$$u(P) = u(P') + \Delta t\, u_t(P') + \frac{\Delta t^2}{2} u_{tt}(P') + O(\Delta t^3).$$

Using (3.1) and (3.2) we can eliminate u_t and h_t on the right hand sides above. Also, differentiating (3.1) and (3.2) with respect to t, we can eliminate u_{tt} and h_{tt} to get finally

$$2. \quad h(P) = h(P') - \Delta t \frac{\partial}{\partial x}(uh)\Big|_{P'} + \frac{\Delta t^2}{2}\frac{\partial}{\partial x}\left[u\frac{\partial(uh)}{\partial x} + h\frac{\partial(\frac{1}{2}u^2+h-H)}{\partial x}\right]_{P'} + O(\Delta t^3)$$

$$3. \quad u(P) = u(P') - \Delta t \frac{\partial}{\partial x}(\tfrac{1}{2}u^2+h-H)\Big|_{P'} + \frac{\Delta t^2}{2}\frac{\partial}{\partial x}\left[\frac{\partial(uh)}{\partial x} + u\frac{\partial(\frac{1}{2}u^2+h-H)}{\partial x}\right]_{P'} + O(\Delta t^3)$$

We now use u, h and H at the points L', P' and R' to approximate the x-derivatives appearing on the right hand sides of (2) and (3). Since the spacing is uniform for points of type I these approximations are easily obtained to accuracy $O(\Delta x^2)$ by using centered difference quotients. For points of type II the spacing is in general non-uniform. However the terms multiplying Δt are first derivatives and so can again be approximated to $O(\Delta x^2)$ using data at three points. The remaining terms are approximated to within $O(\Delta x)$ but since they are multiplied by Δt^2 we retain <u>third order accuracy</u>. One should have no difficulty in deriving the difference equations from the above description.

The difference equations at points of type III, see figure 8c, are identical with those used previously (see eqs. (37) and (38) of [1]). They are difference approximations of the characteristic equation (3.6) centered at the midpoint of the mesh rectangle in figure 8c. Combined with (3.7) these equations yield u(P) and h(P) to third order accuracy.

To fit in the position of the shoreline to higher order accuracy we again note that

$$\xi(t+\Delta t) = \xi(t) + \Delta t\, \dot{\xi}(t) + \frac{\Delta t^2}{2}\, \ddot{\xi}(t) + O(\Delta t^3)$$

However from differentiating (3.4) and using (3.2) at $x = \xi(t)$ we have

4. $$\xi(t) = \left[H(x) - h(x,t)\right]_x \Big|_{x=\xi(t)}$$

so that, recalling (3.4),

5. $$\xi(t+\Delta t) = \xi(t) + \Delta t\, u(\xi(t),t) + \frac{\Delta t^2}{2}\left[H_x(\xi(t) - h_x(\xi(t),t)\right] + O(\Delta t^3)$$

The x-derivatives in (5) can be approximated, using H and h at points P' and R' of figure 8b, to accuracy $O(\Delta x)$ and so if $u(\xi(t),t)$ is computed to accuracy $O(\Delta x^2)$ we get $\xi(t+\Delta t) = \xi(R)$ to third order accuracy. To compute $u(\xi(t+\Delta t),t+\Delta t)$ we use (3.4) and (4) to get:

6. $$u(\xi(t+\Delta t),t+\Delta t) = u(\xi(t),t) + \Delta t\left[H_x(\xi(t)) - h_x(\xi(t),t)\right] + O(\Delta t^2)$$

Thus with the same approximations to x-derivatives used in (5) we obtain $u(R)$, see figure 8b, to second order accuracy.

The stability condition and interpolation procedures (for $\xi_{k+1} > x_{x+1} + \frac{\Delta x}{2}$) of [1] are also employed but we do not repeat them here.

5. Results of the calculations

In all of the calculations we used the uniformly sloping bottom profile (2.3) and uniform x-spacing, $\Delta x = 1/200$. The incident wave function used in (3.7) was

1. $$F(t-1) = a \sin \omega t.$$

Calculations were run for various values of the amplitude a and frequency ω in the following ranges: $10^{-3} \le a \le 8 \times 10^{-3}$, $1 \le \omega \le 10$. Each case was run until at least 10 and perhaps as many as 14 full period waves had reached the shoreline. In most cases all significant transient effects were absent after 5 or 6 periods; however in some cases a steady regime was never attained.

Typical cases in which time harmonic steady states were established are shown in figure 2. In figure 2 graphs of $\xi(t)/a$ are shown for two cases in which $a = 10^{-3}$ and $\omega = 2$ or 7. The steady state periods in these cases are just π or $2\pi/7$. After about the first $1\frac{1}{2}$ cycles of shoreline motion the zeros of $\xi(t)$ have these periods. Significant motion of the shoreline is not observed, in either case, until about $t = 2$. However this is just the time required for a sonic disturbance to propagate from $x = -1$ to $x = 0$ over the bottom profile (2.3); i.e.

$$\int_{-1}^{0} \frac{dx}{c(x)} = \int_{-1}^{0} |x|^{-1/2}\, dx = 2.$$

The fact that the signals actually arrive slightly sooner may be attributed to the effects of the nonlinearity, near the shoreline, which increase the characteristic speed (and to a small numerical effect). These figures also show that the maximum steady state runup distance may be exceeded by some of the initial, transient, runups.

For comparison with the theoretical results we define the computed amplification as

$$2. \qquad A \equiv \max_{T < t < T + \frac{2\pi}{\omega}} \frac{\xi(t)}{a},$$

where T is some "large" time. If this quantity varies slightly with T we may use an average over several periods. In Table I we list this amplification as well as the corresponding minimum shoreline excursion for a variety of cases. When the variation of these quantities over the last three computed periods was not small (say less than 5 %) we list the range of observed variation. Thus, for example, the case $\omega = 8$ and $a = 10^{-3}$ did not quite reach a steady state and the amplification varied between $12.9 \leq A \leq 14.2$ in the last few periods.

The first column of Table I is plotted in figure 3 together with theoretical amplification curves for $\alpha = 0$ and $\alpha = \tan^{-1} 1/10$. The agreement is very good up to $\omega = 6$ (for the $\alpha = 0$ curve) and should be contrasted with the previous calculations (in figure 5 of [1]). As is shown in this figure and in the table, there seems to be some kind of "resonance" near $\omega = 6.5$ since the amplification becomes very large there. (There are lesser oscillations near $\omega = 4$ and $\omega = 5.5$) Beyond this resonance the computed amplification values seem to lie along a curve considerably above the theoretical values of $\alpha = 0$.

Of course as the frequency increases bores will finally form and the present calculations must fail in these cases. For $a = 10^{-3}$ and $\omega = 7$ the results show quite clearly (see figures 2b and 6) that nothing unusual happens and in fact that bores do not yet form. We have shown in figure 4 the frequency at which the calculations seem to indicate that bores form for various values of incident wave amplitude. The criterion used was not the wild oscillations in or unsteady behavior of $\xi(t)/a$ but rather the occurrence of negative values of h in the calculations. This is of course not a precise determination and so the agreement with the theoretical limit of equation (2.10) is quite gratifying.

In figure 5a we show the initial wave, for $\omega = 2$ and $a = 10^{-3}$, as it approaches the shoreline. The amplitude is seen to grow slowly till the wave front reaches the shoreline and then the growth is much more rapid. Less obvious in this figure is the decrease in wavelength due to the increasing local sound speed. Some steady state wave profiles for this case are shown in figure 5b. The arrows attached to the curves indicate the direction of the water velocity at the corresponding locations. (The scale on these figures is such that the bottom profile has slope 10^3 and thus appears almost vertical.)

Figure 6a and 6b show corresponding wave profiles for $\omega = 7$ and $a = 10^{-3}$. The shortening of the wave length is clearly illustrated here. The local wave-length, L, at a position x is, in the linear theory,

$$3. \qquad L(x) = \frac{2\pi}{\omega} c(x) = \frac{2\pi}{\omega} |x|^{1/2}$$

As a rough check we examine the curve in figure 6a for t = 1.765 (or cyle No. 500). Calling the distance between two successive nodes or two local extrema a half wavelength, L/2, and comparing this to the theoretical results (3) evaluated at the midpoint of the two points in question we get:

	x	-.808	-.636	-.475	-.334	-.220	-.124	-.064
L	computations	.710	.716	.619	.494	.400	.346	.226
	linear theory	.807	.716	.620	.519	.422	.317	.227

Somewhat better agreement can be obtained by replacing (3) with average local wavelengths defined in

$$\int_{x-\frac{L(x)}{4}}^{x+\frac{L(x)}{4}} \frac{dx'}{c(x')} = \frac{\pi}{\omega} .$$

ω	$a = 10^{-3}$		$a = 2 \times 10^{-3}$		$a = 4 \times 10^{-3}$		$a = 6 \times 10^{-3}$	
	max	min	max	min	max	min	max	min
1.0	3.23	-3.23						
1.5	4.68	-4.68						
2.0	4.96	-4.97	4.96	-4.98	4.95	-4.99	4.94	-5.00
2.5	5.36	-5.38						
3.0	6.35	-6.36	6.35	-6.47	6.30	-6.42	6.20	-6.48
3.5	6.61	-6.75						
4.0	7.0/7.9	-7.1/-7.7	6.89	-7.00	7.18	-7.13	7.4/7.9	-6.6
4.5	7.69	-7.77						
5.0	7.87	-8.07	7.70	-8.15	11.2/18	-7/-10.5	8.2/30	-3.4/-18.7
5.5	7.0/8.2	-8.4						
6.0	8.21	-9.45	12.4/14.3	-8.1/-9.3	5.8/33	-4.2/-22		
6.5	25/125	-22/-70						
7.0	11.8	-8.5	50/53	-28/-30				
7.5	12.4	-9.3						
8.0	12.9/14.2	-9.1/10.4						
9.0	5.4/44	-14/-47						
10.0	43/80	-18/-43						

Table I

Maximum and minimum shoreline excursions in "steady" state $\left[\text{i.e. } \max\limits_{T<t<T+P} \frac{\xi(t)}{a}\right.$ and $\min\limits_{T<t<T+P} \frac{\xi(t)}{a}$ for T "large" and P at least a period$\left.\right]$.

6. The breaking of waves

The theory of wave amplification reviewed in section 2 concerns the case in which the waves do not break and bores do not form. But the excluded case is the most important one in the study of tsunamis, since experience shows that they always form bores. Therefore we shall now present a theory of wave breaking with the consequent formation and growth of a bore. We shall base our analysis on the nonlinear shallow water theory, assuming the motion to be in a plane and the bottom to slope uniformly. The main mathematical technique to be used is the theory of characteristics, which will be combined with the theory of weak shock waves.

A qualitative description of wave breaking based on the nonlinear shallow water theory was given by H. Jeffreys in 1934. It is that the higher parts of a wave travel faster than the lower parts so that the wave steepens as it propagates and ultimately breaks. This explanation was repeated by J. J. Stoker [3] and illustrated by the calculation of a wave profile at successive instants, showing how it steepens. Stoker also calculated the time and place at which the profile becomes vertical at some point, which is the time and place at which breaking may be said to occur. These calculations were for waves in water of constant depth.

In this section we shall also calculate the wave profile at successive instants, and determine the time and place at which breaking occurs, for waves on a uniformly sloping beach. In the next section we shall determine the manner in which the height of the resulting bore grows as it propagates toward shore.

We begin by writing the equations of the nonlinear shallow water theory in characteristic form as follows

1. $(u + 2c)_t + (u + c)(u + 2c)_x - gh_x = 0$

2. $(u - 2c)_t + (u - c)(u - 2c)_x - gh_x = 0$

For a uniformly sloping bottom h_x is constant. Therefore we write $gh_x = -m$ where m is a positive constant. Now (1) and (2) can be integrated with the result (see [3], p. 294)

3. $u + 2c + mt = k_+ = \text{const.}$ on C_+ defined by $\frac{dx}{dt} = u + c$

4. $u - 2c + mt = k_- = \text{const.}$ on C_- defined by $\frac{dx}{dt} = u - c$

The curves C_+ and C_- are called characteristics.

From (3) and (4) we find

5. $u = \frac{1}{2}(k_+ + k_-) - mt$

6. $c = \frac{1}{4}(k_+ - k_-)$

Now the equations for the characteristics can be written

7. $\frac{dx}{dt} = \frac{3}{4} k_+ + \frac{1}{4} k_- - mt$ on C_+

8. $\frac{dx}{dt} = \frac{1}{4} k_+ + \frac{3}{4} k_- - mt$ on C_-

The constants k_+ and k_- can be determined from (3) and (4) if the values of u and c are known at some point on each characteristic. For example at the shoreline $x = \xi(t)$, we know that $c = 0$ and $u = d\xi/dt$. Therefore if a characteristic touches the shoreline at $t = t_s$, we have on it

9. $$k_{\pm} = mt_s + \frac{d\xi(t_s)}{dt}$$

If the shoreline is at rest, (9) becomes

10. $$k_{\pm} = mt_s$$

In a region of the water which is undisturbed we have $u = 0$ and $c = \sqrt{-mx}$. Therefore the undisturbed characteristics satisfy the equation

11. $$\frac{dx}{dt} = \pm \sqrt{-mx} \qquad \text{on } C_{\pm}$$

The solutionsof (11) are

12. $$t - t_o = \pm \frac{2}{m}\left[(-mx_o)^{1/2} - (-mx)^{1/2}\right] \qquad \text{on } C_{\pm}$$

Let us now consider a C_+ characteristic which crosses a family of C_- characteristics all of which have come from the undisturbed shoreline $\xi(t) = 0$. Then from (10), $k_- = mt_s$ on them so (5)-(7) become

13. $$u = \frac{1}{2}(k_+ + mt_s) - mt$$

14. $$c = \frac{1}{4}(k_+ - mt_s)$$

15. $$\frac{dx}{dt} = \frac{3}{4} k_+ + m\left(\frac{t_s}{4} - t\right)$$

We now make the basic assumption of the theory of weak waves, which is that the C_- characteristics are undisturbed. Then their equations are given by (12) with the lower sign. Since they touch the undisturbed shoreline, we may set $t_o = t_s$ and $x_o = 0$ in (12). In this way we get t_s in terms of x and t. Then by using this expression for t_s we can rewrite (13)-(15) as

16. $$u = \frac{1}{2} k_+ - \frac{mt}{2} - (-mx)^{1/2}$$

17. $$c = \frac{1}{4} k_+ - \frac{mt}{4} + \frac{1}{2}(-mx)^{1/2}$$

18. $$\frac{dx}{dt} = \frac{3}{4} (k_+ - mt) - \frac{1}{2}(-mx)^{1/2}$$

To solve (18) we introduce τ and $z(\tau)$ defined by

19. $$\tau = mt - k_+, \qquad z(\tau) = (-mx)^{1/2}$$

Then (18) becomes

20. $$\frac{dz}{d\tau} = \frac{3}{8} \frac{\tau}{z} + \frac{1}{4}$$

Since (20) is a homogeneous equation, it can be solved by introducing $u(\tau)$ defined by

21. $$u(\tau) = \tau^{-1} z(\tau)$$

In terms of u, (20) becomes

22. $$\tau \frac{du}{d\tau} = \frac{3}{8u} + \frac{1}{4} - u$$

The variables are separated in (22) so it can be integrated to yield

23. $$\tau^{-1} = A_1(u - \frac{3}{4})^{3/5} (u + \frac{1}{2})^{2/5}$$

Here A_1 is an arbitrary constant.

Upon eliminating u by means of (21) and simplifying, we can write (23) as

24. $$(z - \frac{3\tau}{4})^3 (z + \frac{\tau}{2})^2 = A$$

Here A is another constant. In terms of t and x, (24) becomes

25. $$\left[(-mx)^{1/2} - \frac{3mt}{4} + \frac{3k_+}{4}\right]^3 \left[(-mx)^{1/2} + \frac{mt}{2} - \frac{k_+}{2}\right]^2 = A$$

The constant A can be expressed in terms of some point x_o, t_o on the characteristic, and (25) can be rewritten as

26. $$\left[(-mx)^{1/2} - \frac{3mt}{4} + \frac{3k_+}{4}\right]^3\left[(-mx)^{1/2} + \frac{mt}{2} - \frac{k_+}{2}\right]^2 =$$

$$= \left[(-mx_o)^{1/2} - \frac{3mt_o}{4} + \frac{3k_+}{4}\right]^3\left[(-mx_o)^{1/2} + \frac{mt_o}{2} - \frac{k_+}{2}\right]^2$$

The constant k_+ is given by (3) in terms of the values of u and c at (x_o, t_o) as

27. $$k_+ = u(x_o,t_o) + 2c(x_o,t_o) + mt_o$$

Thus u and c at any point (x,t) satisfying (26) are given by (16) and (17), with k_+ given by (27).

To solve (26) for x in terms of t, we first define $f_1(x_o,t_o)$ and $f(x_o,t_o)$ by

28. $$c(x_o,t_o) = (-mx_o)^{1/2} + f(x_o,t_o)$$

29. $$f(x_o,t_o) = u(x_o,t_o) + 2f_1(x_o,t_o)$$

Now if $f(x_o,t_o) = 0$ the squared term on the right side of (26) vanishes. By equating to zero the squared term on the left side of (26) we rederive the equation (12) for an undisturbed C_+ characteristic.

Now let us suppose that $f(x_o,t_o)$ is not necessarily zero, but is small. Then we may expect the characteristic (26) to differ only slightly from the undisturbed characteristic (12). Therefore we shall try to express it in the form

30. $$t - t_o = \frac{2}{m}[(-mx_o)^{1/2} - (-mx)^{1/2}] + q$$

Here q is to be determined by substituting (30) into (26). By keeping terms of the zeroth and first powers in $f(x_o,t_o)$ we find that

$$31. \qquad q = -\frac{1}{m} f(x_o,\, t_o)\left[\left(\frac{x_o}{x}\right)^{3/4} - 1\right]$$

Thus for small motions, the C_+ characteristic is given by

$$32. \qquad t-t_o = \frac{2}{m}\left[(-mx_o)^{1/2}-(-mx)^{1/2}\right] - \frac{1}{m} f(x_o,t_o)\left[\left(\frac{x_o}{x}\right)^{3/4} - 1\right]$$

We may now use (32) in (16) and (17) to obtain u and c on the C_+ characteristic (32), with the results

$$33. \qquad u(x,t) = \frac{1}{2} f(x_o,t_o)\left(\frac{x_o}{x}\right)^{3/4}$$

$$34. \qquad c(x,t) = (-mx)^{1/2} + \frac{1}{2} f(x_o,t_o)\left(\frac{x_o}{x}\right)^{3/4}$$

These results are not valid near $x = 0$ because there it is not correct to omit higher order terms, as was done in deriving (31). In fact the full expression (26) for the C_+ characteristic leads to finite values of u and c everywhere including $x = 0$.

It is easy to see from (32)-(34) that wave crests steepen in front and become vertical as they approach shore. To show this, let us evaluate $u_x(x,t)$ assuming that the initial values of u and c are given on the line x_o = constant. Then from (33) we have

$$35. \qquad u_x(x,t) = -\frac{3}{8} f(x_o,t_o)x_o^{3/4}\, x^{-7/4} + \frac{1}{2} f_{t_o}(x_o,t_o)(x_o/x)^{3/4}\frac{dt_o}{dx}$$

Now from (32) we find

$$36. \qquad -\frac{dt_o}{dx} = (-mx)^{-1/2} + \frac{3}{4m} f(x_o,t_o) x_o^{3/4} x^{-7/4} - \frac{1}{m} f_{t_o}(x_o,t_o) \left[\left(\frac{x_o}{x} \right)^{3/4} - 1 \right] \frac{dt_o}{dx}$$

Solving (36) for dt_o/dx yields

$$37. \qquad \frac{dt_o}{dx} = \left\{ \frac{1}{m} f_{t_o} \left[(x_o/x)^{3/4} - 1 \right] - 1 \right\}^{-1} \left\{ (-mx)^{-1/2} + \frac{3f x_o^{3/4} x^{-7/4}}{4m} \right\}$$

We see from (37) that dt_o/dx becomes infinite when the denominator vanishes which occurs if $u_{t_o} + 2f_{t_o} > 0$. Then from (35), u_x also becomes ininite. The value of x at which this occurs is found from (37) to be

$$38. \qquad x = x_o \left[1 + \frac{m}{f_{t_o}} \right]^{-4/3}$$

The time at which this occurs is obtained from (32) by inserting the value (38) for x. The first occurrence of an infinite value of u_x is determined by the value of t_o which minimizes t. Exactly the same type of consideration applies if the initial values of u and c are given at t_o = constant or on any other curve in the x_o, t_o plane.

When u_x becomes infinite, c_x also becomes infinite. The first occurrence of this vertical slope for a given wave is called breaking of the wave. Thereafter the solution (32)-(34) is multiple valued. This multiple valuedness can be eliminated by the introduction of a discontinuity, called a bore, into the subsequent wave profile. We shall now show how this is to be done.

7. The formation and growth of bores.

A bore is a discontinity in water depth and velocity across which two jump conditions must be satisfied. These are the mass and momentum equations which may be written in the form

1. $$(\eta_1 + h)(u_1 - \dot{s}) = (\eta_2 + h)(u_2 - \dot{s})$$

2. $$(\eta_1+h)u_1(u_1-\dot{s})+ \frac{g}{2}(\eta_1+h)^2 = (\eta_2+h)u_2(u_2-\dot{s})+ \frac{g}{2}(\eta_2+h)^2$$

Here η_1 and u_1 denote the wave height and water velocity on side one of the bore, $\dot{s}$ is the bore velocity and η_2, u_2 denote quantities on side two. From (1) and (2) we find for a weak bore, i.e., one for which $|\eta_1-\eta_2| \ll h$,

3. $$\dot{s} = u_2 \pm \sqrt{gh}\left[1 + \frac{3\eta_1-\eta_2}{4h} + \ldots\right]$$

4. $$u_1 = u_2 \pm \sqrt{gh}\left(\frac{\eta_1-\eta_2}{h}\right) + \ldots$$

If the fluid crosses the bore from side two to side one, the plus sign applies in (3) and (4), and side two is called the front.

When side two is the front, we find from the definition of c and from (4) that

5. $$c_1+u_1+c_2+u_2 = 2\left[u_2 + \sqrt{gh}\left(1 + \frac{3\eta_1-\eta_2}{4} + \ldots\right)\right]$$

Upon comparing (5) with (3) in which the plus sign is chosen, we find that

6. $$\dot{s} = \frac{1}{2}(c_1+u_1+c_2+u_2) + \dots = \frac{1}{2}\left(\frac{dx_1}{dt} + \frac{dx_2}{dt}\right) + \dots$$

Thus the speed of a weak bore is the average of the C_+ characteristic speeds on its two sides. This result also holds in gas dynamics and in certain other cases.

The expression (6) for the velocity of the bore, together with the expression (6.32) for the C_+ characteristics suffices for the determination of the location of the bore as a function of time. To determine the bore location we again use the notation $z = (-mx)^{1/2}$ and we also introduce $\sigma = \frac{mt}{2}$. We assume that the incident wave is given at $x = x_o$ which corresponds to $z = z_o$. Suppose that two C_+ characteristics which leave $x = x_o$ at $t = t_1$ and $t = t_2$ with $t_1 > t_2$, meet at the bore. The equations of these characteristics are given by (6.32) with t_o replaced by t_1 or t_2. In terms of z and σ these equations are

7. $$\sigma + z - z_o = \sigma_1 - \frac{1}{2} f(\sigma_1)\left[(z_o/z)^{3/2} - 1\right]$$

8. $$\sigma + z - z_o = \sigma_2 - \frac{1}{2} f(\sigma_2)\left[(z_o/z)^{3/2} - 1\right]$$

Here $f(\sigma_1)$ denotes $f(x_o,t_1)$.

Let us write the equation of the bore in the form

9. $$\sigma + z - z_o = G(z)$$

To determine G(z) we first combine (7) and (8) with (9) to obtain

10. $$G(z) = \sigma_1 - \frac{1}{2} f(\sigma_1)\left[(z_o/z)^{3/2}-1\right]$$

11. $$G(z) = \sigma_2 - \frac{1}{2} f(\sigma_2)\left[(z_o/z)^{3/2}-1\right]$$

Next we wish to utilize (6). Before doing so we observe, from the definitions of z and σ, that

12. $$\dot{s} = \frac{dx}{dt} = -\frac{2z}{m}\frac{dz}{dt} = -z\frac{dz}{d\sigma}$$

Now from (9)

13. $$\frac{dz}{d\sigma} = \frac{1}{G'(z)-1} \qquad -1 - G'(z)$$

Thus (12) and (13) yield

14. $$\dot{s} = z\left[1 + G'(z)\right]$$

To obtain dx_1/dt and dx_2/dt we differentiate (7) and (8) to find

15. $$\frac{dx_1}{dt} = -z\frac{dz_1}{d\sigma} = -z\{-1+\tfrac{3}{4}f(\sigma_1)z_o^{3/2}z^{-5/2}\}^{-1} \approx z\{1+\tfrac{3}{4}f(\sigma_1)z_o^{3/2}z^{-5/2}\}$$

16. $$\frac{dx_2}{dt} = -z\frac{dz_2}{d\sigma} = -z\{-1+\tfrac{3}{4}f(\sigma_2)z_o^{3/2}z^{-5/2}\}^{-1} \approx z\{1+\tfrac{3}{4}f(\sigma_2)z_o^{3/2}z^{-5/2}\}$$

Upon using (14)-(16) in (6) we obtain

17. $$2G'(z) = \tfrac{3}{4}z_o^{3/2}z^{-5/2}\left[f(\sigma_1)+f(\sigma_2)\right]$$

The problem is now that of solving (10),(11) and (17) for σ_1, σ_2 and G as functions of z. To solve this problem we follow the method of G. B. Witham [4]. We differentiate (10) and (11) with respect to z and add the results, obtaining

18. $$2G'(z) = \tfrac{3}{4}z_o^{3/2}z^{-5/2}\left[f(\sigma_1)+f(\sigma_2)\right] + \frac{d\sigma_1}{dz}\{1-\tfrac{1}{2}f'(\sigma_1)\left[(z_o/z)^{3/2}-1\right]\}$$
$$+\frac{d\sigma_2}{dz}\{1-\tfrac{1}{2}f'(\sigma_2)\left[(z_o/z)^{3/2}-1\right]\}$$

By taking account of (17), we can simplify (18) to

$$19. \qquad \frac{d\sigma_1}{dz}\left\{1 - \frac{f'(\sigma_1)}{2}\left[(z_o/z)^{3/2}-1\right]\right\} + \frac{d\sigma_2}{dz}\left\{1 - \frac{f'(\sigma_2)}{2}\left[(z_o/z)^{3/2}-1\right]\right\} = 0$$

To eliminate z from (19) we subtract (11) from (10) and find

$$20. \qquad (z_o/z)^{3/2} - 1 = \frac{2(\sigma_1 - \sigma_2)}{f(\sigma_1)-f(\sigma_2)}$$

Now (19) can be rewritten as

$$21. \qquad \frac{d\sigma_1}{dz}\left\{1 - f'(\sigma_1)\frac{\sigma_1 - \sigma_2}{f(\sigma_1)-f(\sigma_2)}\right\} + \frac{d\sigma_2}{dz}\left\{1 - f'(\sigma_2)\frac{\sigma_1 - \sigma_2}{f(\sigma_1)-f(\sigma_2)}\right\} = 0$$

It is convenient to multiply (21) by $f(\sigma_1)-f(\sigma_2)$ and then to rearrange it in the form

$$22. \qquad f(\sigma_2)\frac{d\sigma_2}{dz} - f(\sigma_1)\frac{d\sigma_1}{dz} = \frac{1}{2}\frac{d}{dz}\left\{\left[\sigma_2-\sigma_1\right]\left[f(\sigma_2)+f(\sigma_1)\right]\right\}$$

Integration of (22) yields

$$23. \qquad \int_{\sigma_1}^{\sigma_2} f(\sigma)d\sigma = \frac{1}{2}(\sigma_2-\sigma_1)\left[f(\sigma_2)+f(\sigma_1)\right]$$

The constant of integration in (23) has been chosen so that (23) is satisfied by $\sigma_1 = \sigma_2$, which corresponds to the first point on the path of the bore. The condition (23) determines the correspondence between σ_1 and σ_2. The geometrical interpretation of (23) is that the area bounded by the curve $f(\sigma)$, the σ-axis and the lines $\sigma = \sigma_1$ and $\sigma = \sigma_2$ is equal to the area of the trapezoid with vertices at $[\sigma_1, f(\sigma_1)]$, $[\sigma_2, f(\sigma_2)]$, $[\sigma_1, 0]$ and $[\sigma_2, 0]$. Alternatively we may say that the signed area between the curve $f(\sigma)$ and the chord from $[\sigma_1, f(\sigma_1)]$ to

$[\sigma_2, f(\sigma_2)]$ is zero. Thus the chord must cut off equal areas on the two sides of the curve.

Once σ_2 is determined as a function of σ_1 from (23), the path of the bore is found by eliminating G(z) from (9) and (10) to obtain

24. $$\sigma-\sigma_1+ z- z_o = - \frac{1}{2} f(\sigma_1)\left[(z_o/z)^{3/2} - 1\right]$$

Now z is given in terms of σ_1 and σ_2 by (20). Thus (20) and (24) are parametric equations for the path of the bore with σ_1 as parameter. These equations may be written more explicitly in the form

25. $$z = z_o\left[1 + \frac{2(\sigma_1 - \sigma_2)}{f(\sigma_1)-f(\sigma_2)}\right]^{-2/3}$$

26. $$\sigma = \sigma_1+ z_o - z - f(\sigma_1) \frac{\sigma_1 - \sigma_2}{f(\sigma_1)-f(\sigma_2)}$$

The discontinuities in u and c can be found from (6.33) and (6.34). They are

27. $$u_1-u_2 = \frac{1}{2} \left(\frac{z_o}{z}\right)^{3/2} \left[f(\sigma_1)-f(\sigma_2)\right]$$

28. $$c_1-c_2 = \frac{1}{2}\left(\frac{z_o}{z}\right)^{3/2} \left[f(\sigma_1)-f(\sigma_2)\right]$$

By using (20) we may rewrite these results as

29. $$u_1- u_2 = c_1- c_2 = \sigma_1- \sigma_2+ \frac{1}{2}\left[f(\sigma_1)-f(\sigma_2)\right]$$

The equation (23) can be solved readily for σ_2 in terms of σ_1 if $f(\sigma)$ is an odd function, i.e., if

30. $f(-\sigma) = -f(\sigma)$

It is then easy to see that the solution of (23) is

31. $\sigma_2 = -\sigma_1$

Then (25), (26) and (29) become

32. $$z = z_o\left[1 + \frac{2\sigma_1}{f(\sigma_1)}\right]^{-2/3}$$

33. $\sigma = z_o - z$

34. $u_1-u_2 = c_1-c_2 = 2\sigma_1 + f(\sigma_1)$

To illustrate the results (32)-(34) let us apply them to a sinusoidal incident wave for which

35. $f(\sigma) = A \sin\left(\frac{2\pi\sigma}{T}\right)$

Then (32) and (34) become

36. $$z = z_o\left[1 + \frac{2\sigma_1}{A \sin\left(\frac{2\pi\sigma_1}{T}\right)}\right]^{-2/3}$$

37. $u_1 - u_2 = c_1 - c_2 = 2\sigma_1 + A \sin\left(\frac{2\pi\sigma_1}{T}\right)$

We can simplify these formulas by introducing in place of σ_1 the parameter δ defined by

38. $$\delta = \frac{2\pi\sigma_1}{T}$$

Then (36) and (37) become

39. $$z = z_o\left[1 + \frac{T}{\pi A} \cdot \frac{\delta}{\sin \delta}\right]^{-2/3}$$

40. $$u_1 - u_2 = c_1 - c_2 = A\left[\frac{T}{\pi A}\,\delta + \sin \delta\right]$$

From (39) we find that the bore forms at $z = z_o(1+ \frac{T}{\pi A})^{-2/3}$ where $\delta = 0$ and travels toward the shore $z = 0$ which it reaches when $\delta = \pi$. From (33) we see that the bore path is an undisturbed C_+ characteristic starting at $\sigma = z_c - z_o(1+ \frac{T}{\pi A})^{-2/3}$ and reaching the shore at $\sigma = z_o$. The maximum discontinuity across the bore occurs at $\delta = \cos^{-1}(-T/\pi a)$ provided $T/\pi A < 1$, and its value is

41. $$u_1 - u_2 = c_1 - c_2 = A\left\{\frac{T}{\pi A} \cos^{-1}\left(\frac{-T}{\pi A}\right) + \left[1 - \left(\frac{T}{\pi A}\right)^2\right]^{1/2}\right.$$

If $T/\pi A > 1$, the maximum discontinuity occurs at $\delta = \pi$ i.e., at the undisturbed shoreline, and its magnitude is T. In terms of the original variables $T = \frac{gT_o \tan \alpha}{2}$ where α is the beach angle and T_o is the period of the incident wave.

When $T > \pi A$ the ratio of the maximum bore discontinuity to the incident amplitude is $T/A = gT_o \tan \alpha/2A$. Thus this factor, which we may call the velocity amplification, increases with the period of the wave and with the beach angle.

References

[1] J. B. Keller and H. B. Keller, Water wave run-up on a beach, Research report issued June 1964 by the Service Bureau Corp., N.Y., N.Y. to the Office of Naval Research, Dept. of the Navy, Wash. D. C.

[2] P. D. Lax and B. Wendroff, Difference schemes for hyperbolic equations with high order of accuracy, Comm. Pure Appl. Math., 17 (1964) 381-398.

[3] J. J. Stoker, Water waves. Interscience Publ. Inc., New York (1957).

[4] G. B. Whitham, The flow pattern of a supersonic projectile, Comm. Pure. Appl. Math., 5 (1952), 301-348.

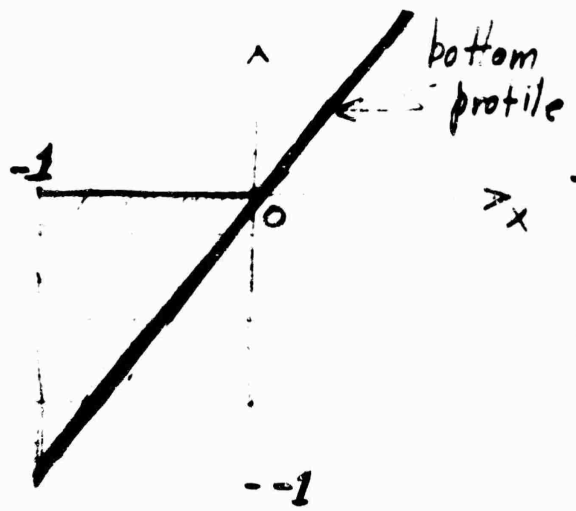

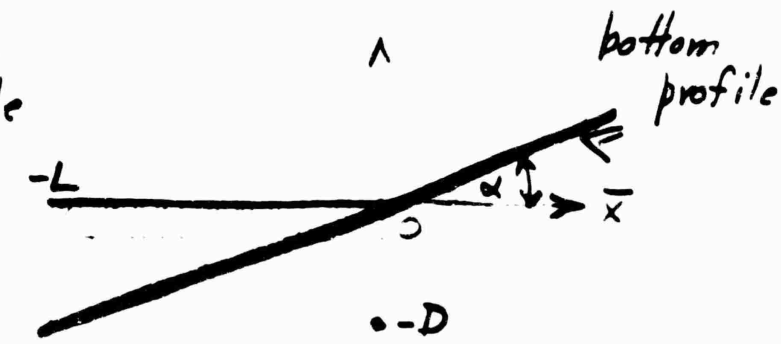

Fig 1a. Initial configuration in dimensionless variables.

Fig. 1b. Initial configuration in dimensional variables.

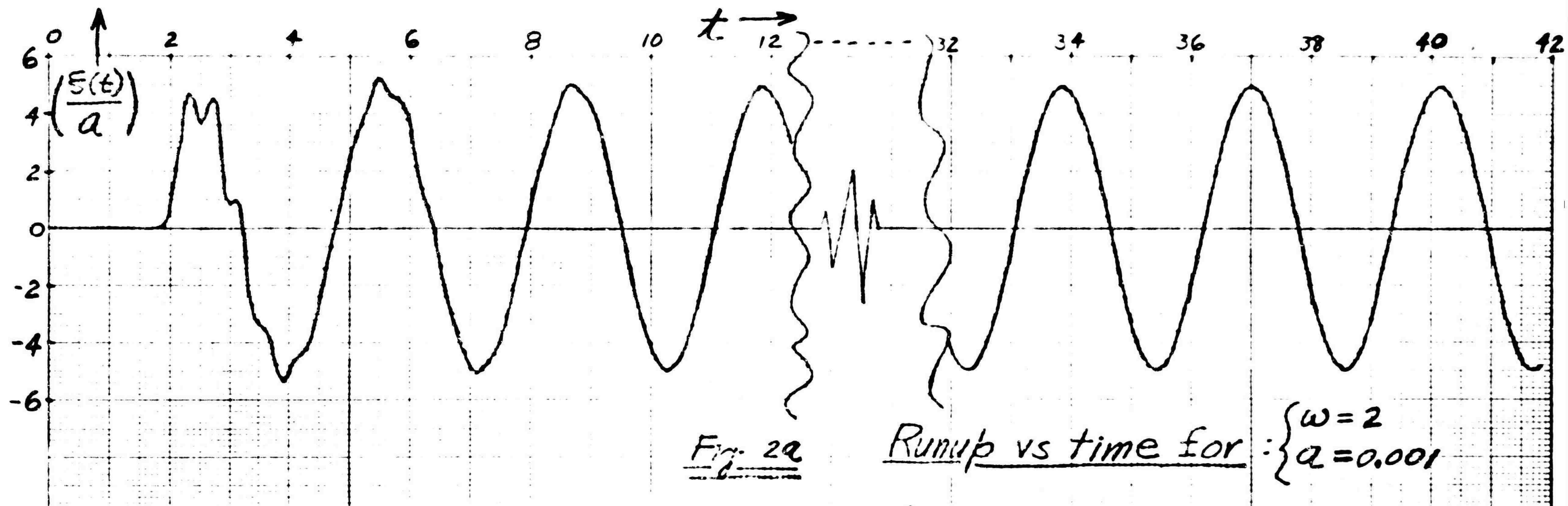

Fig. 2a Runup vs time for: $\begin{cases} \omega = 2 \\ a = 0.001 \end{cases}$

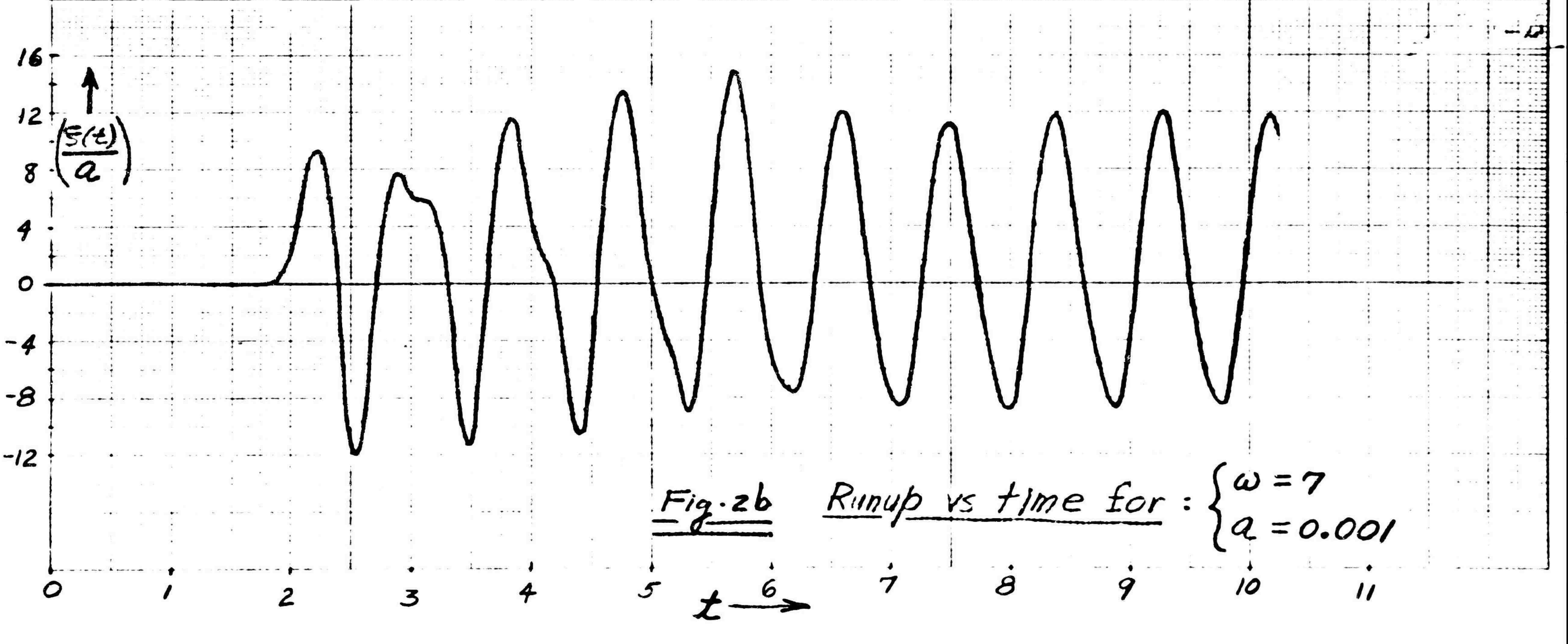

Fig. 2b Runup vs time for: $\begin{cases} \omega = 7 \\ a = 0.001 \end{cases}$

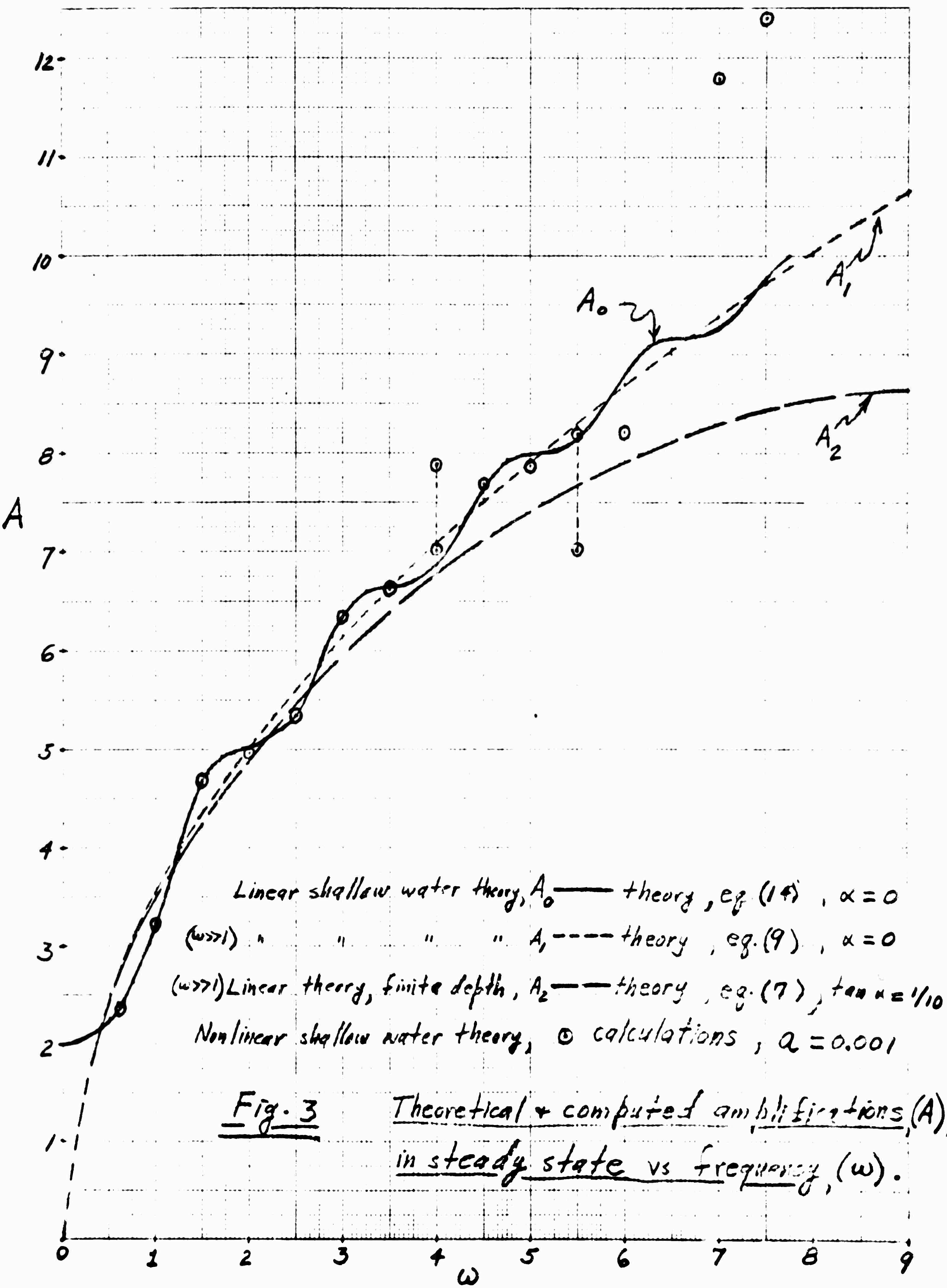

Fig. 3 Theoretical + computed amplifications (A) in steady state vs frequency, (ω).

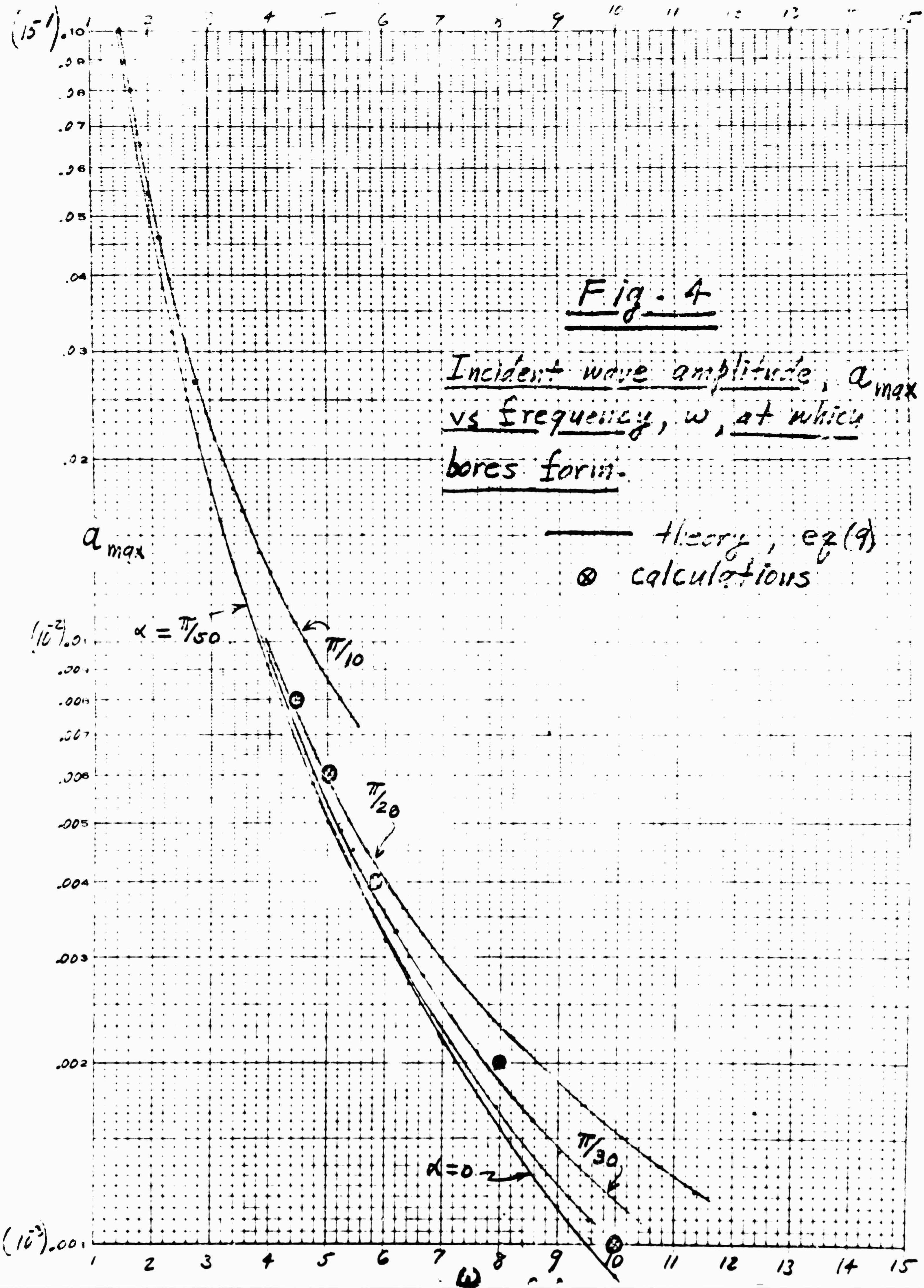
Fig. 4
Incident wave amplitude, a_{max}, vs frequency, ω, at which bores form.
—— theory, eq (9)
⊗ calculations
a_{max}
ω
$\alpha = \pi/50$
$\pi/10$
$\pi/20$
$\pi/30$
$\alpha=0$
(10^{-1}) .10
(10^{-2}) .01
(10^{-3}) .001
.02
.03
.04
.05
.002
.003
.004
.005
1
2
3
4
5
6
7
8
9
10
11
12
13
14
15

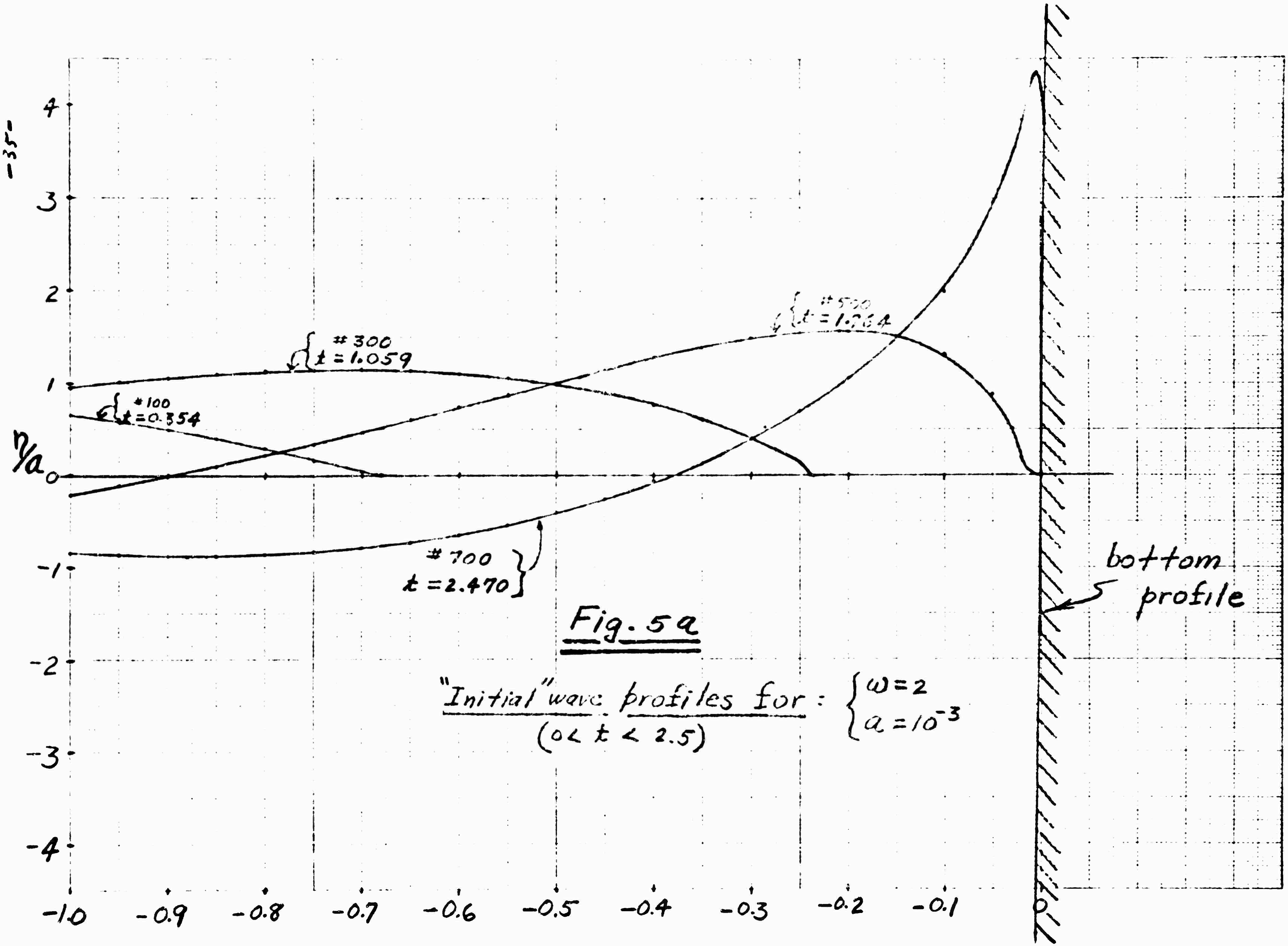

Fig. 5a

"Initial" wave profiles for: $\begin{cases} \omega = 2 \\ a = 10^{-3} \end{cases}$

$(0 < t < 2.5)$

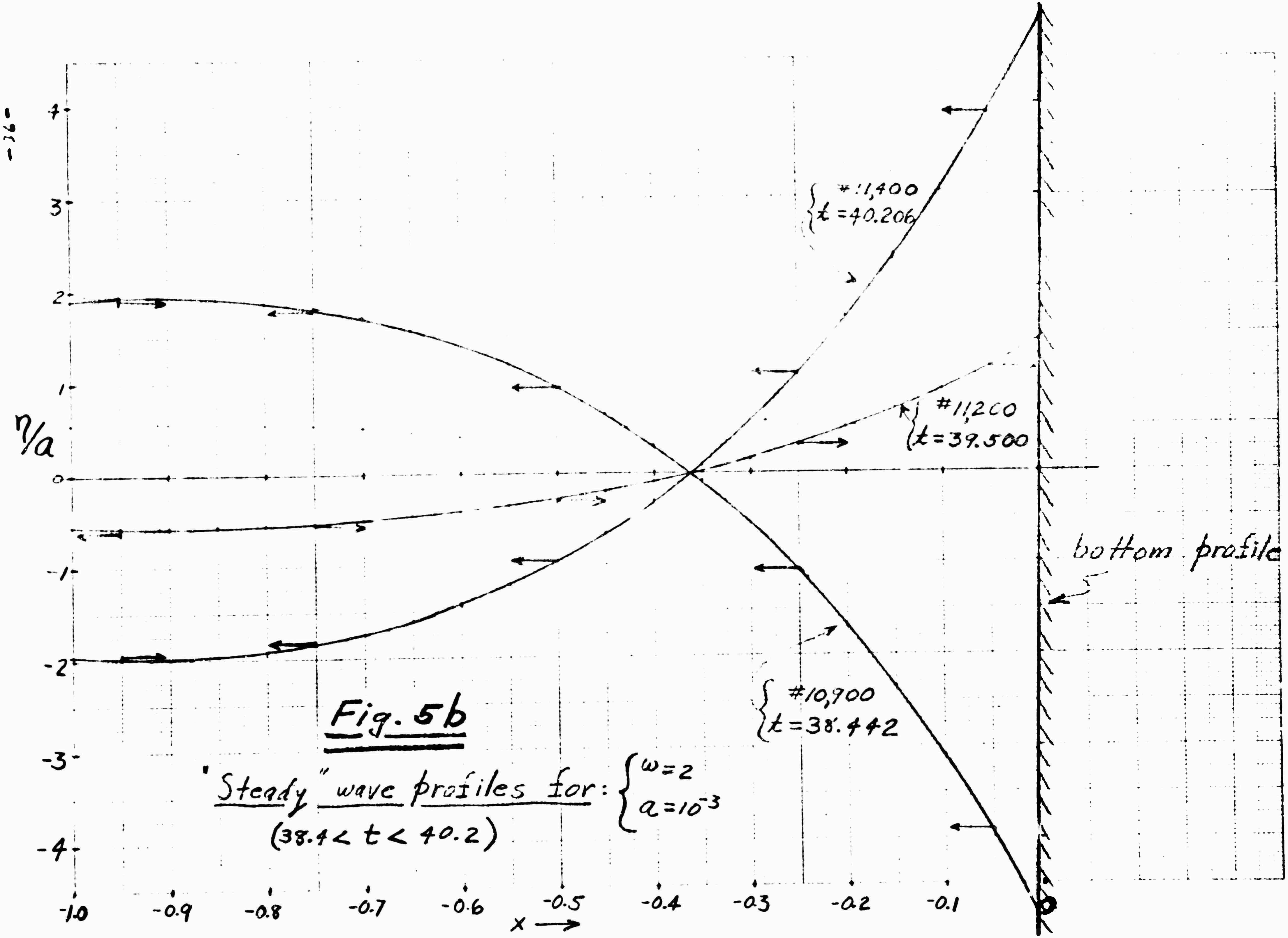

Fig. 5b

"Steady" wave profiles for: $\begin{cases} \omega = 2 \\ a = 10^{-3} \end{cases}$

$(38.4 < t < 40.2)$

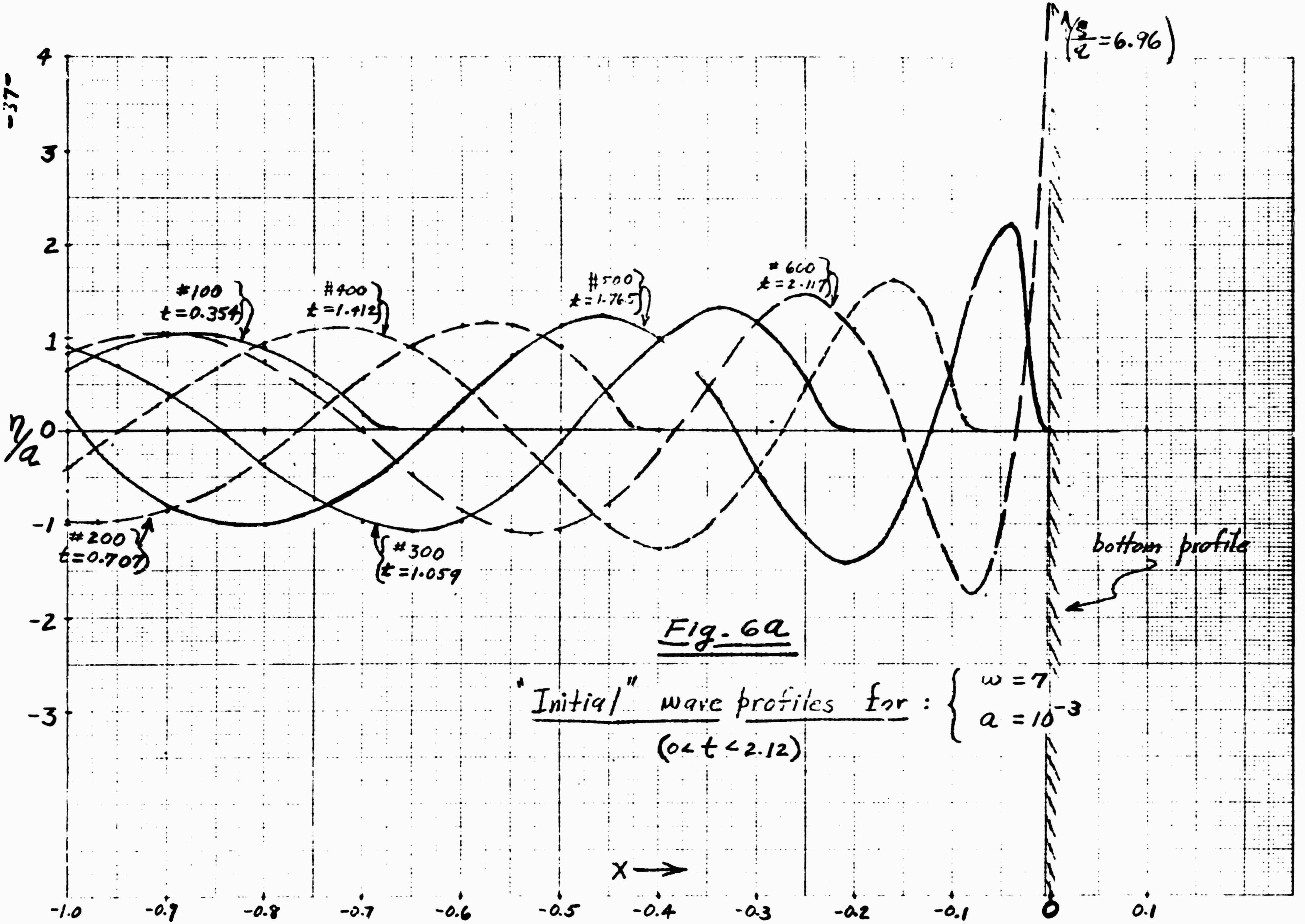

Fig. 6a

"Initial" wave profiles for : $\begin{cases} \omega = 7 \\ a = 10^{-3} \end{cases}$

$(0 < t < 2.12)$

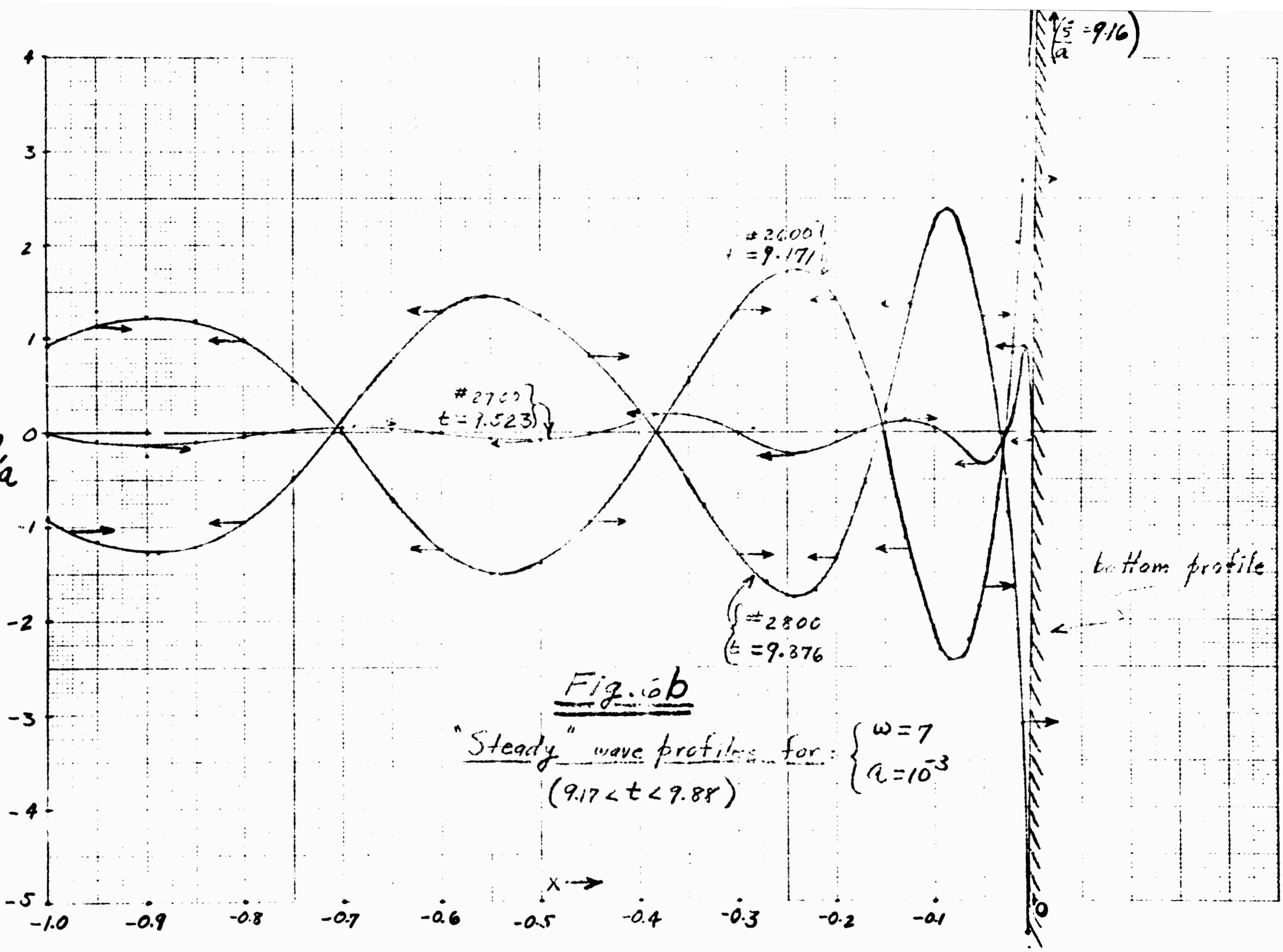

Fig. 10b

"Steady" wave profiles for: $\left\{ \begin{array}{l} \omega = 7 \\ a = 10^{-3} \end{array} \right.$

$(9.17 < t < 9.88)$

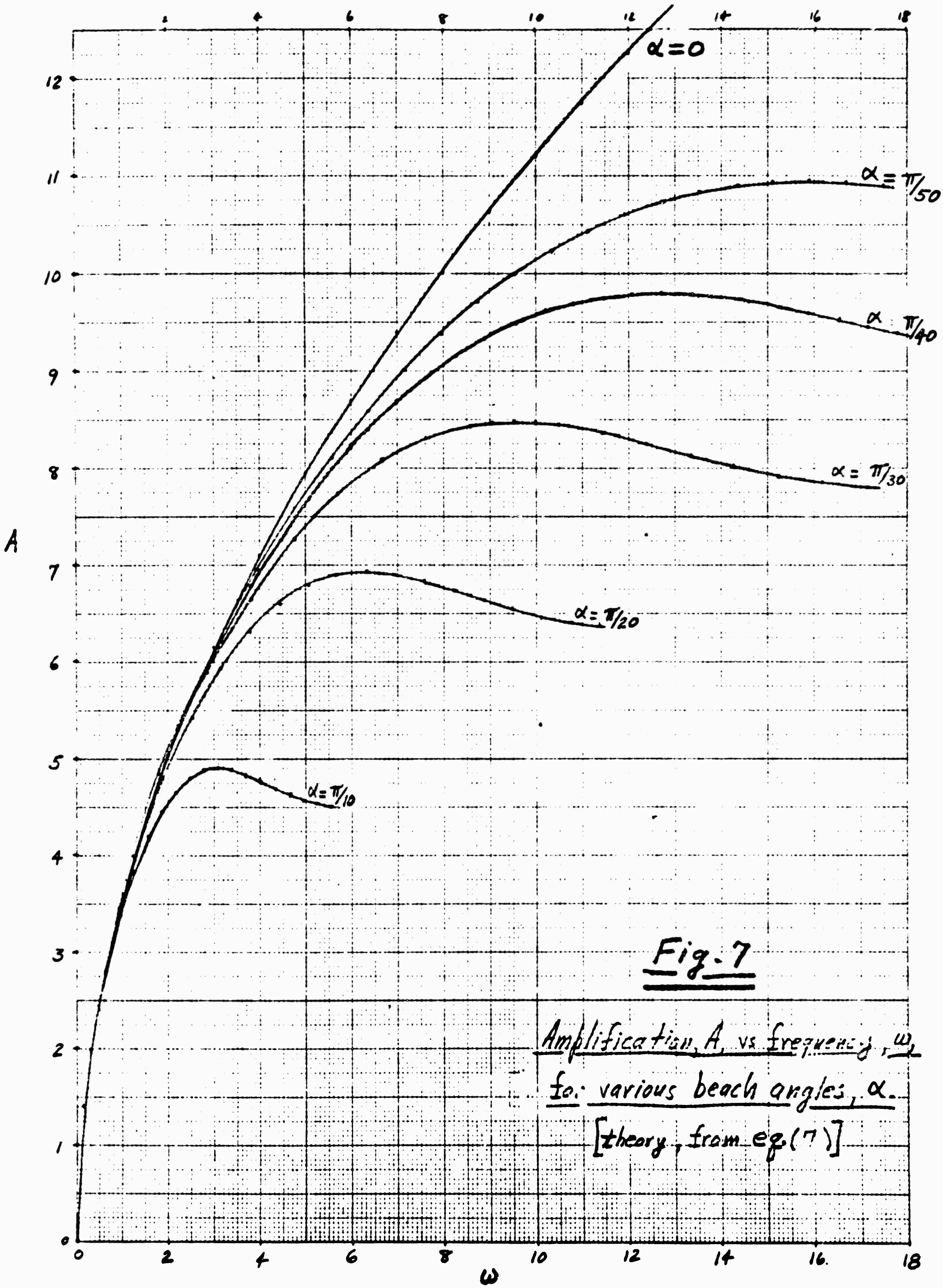

Fig. 7

Amplification, A, vs frequency, ω, for various beach angles, α.
[theory, from eq. (7)]

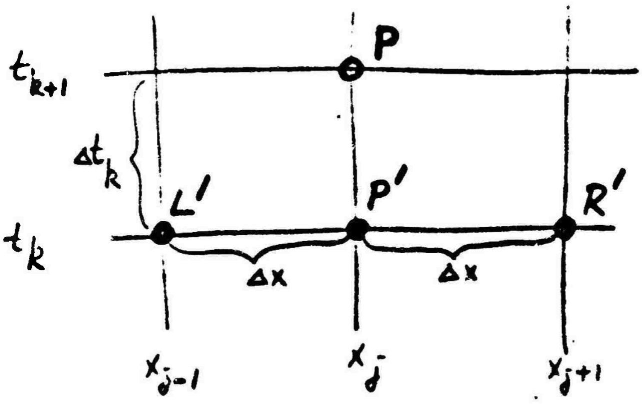

Fig 8a. "Interior" net points of type I for calculations at P.

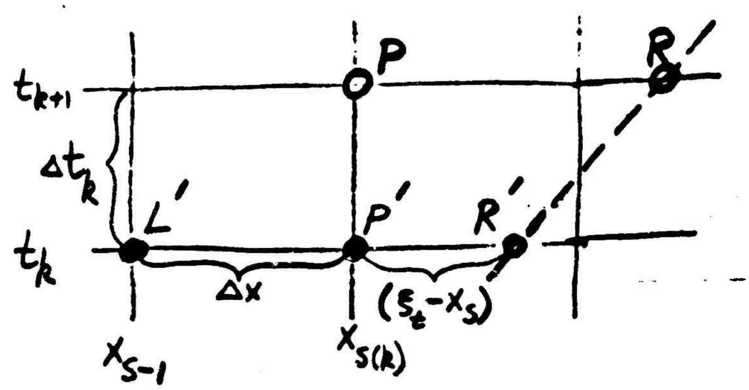

Fig 8b. Shoreline points of types II and IV for calculations at P and R

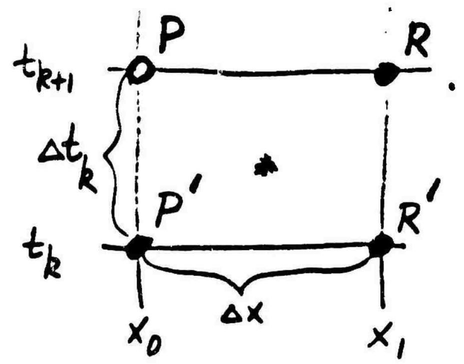

Fig 8c. "Incident" wave points of type III for calculations at P.